
Princeton Plasma Physics Laboratory

PPPL-

PPPL-



Prepared for the U.S. Department of Energy under Contract DE-AC02-09CH11466.

Princeton Plasma Physics Laboratory

Report Disclaimers

Full Legal Disclaimer

This report was prepared as an account of work sponsored by an agency of the United States Government. Neither the United States Government nor any agency thereof, nor any of their employees, nor any of their contractors, subcontractors or their employees, makes any warranty, express or implied, or assumes any legal liability or responsibility for the accuracy, completeness, or any third party's use or the results of such use of any information, apparatus, product, or process disclosed, or represents that its use would not infringe privately owned rights. Reference herein to any specific commercial product, process, or service by trade name, trademark, manufacturer, or otherwise, does not necessarily constitute or imply its endorsement, recommendation, or favoring by the United States Government or any agency thereof or its contractors or subcontractors. The views and opinions of authors expressed herein do not necessarily state or reflect those of the United States Government or any agency thereof.

Trademark Disclaimer

Reference herein to any specific commercial product, process, or service by trade name, trademark, manufacturer, or otherwise, does not necessarily constitute or imply its endorsement, recommendation, or favoring by the United States Government or any agency thereof or its contractors or subcontractors.

PPPL Report Availability

Princeton Plasma Physics Laboratory:

<http://www.pppl.gov/techreports.cfm>

Office of Scientific and Technical Information (OSTI):

<http://www.osti.gov/bridge>

Related Links:

[U.S. Department of Energy](#)

[Office of Scientific and Technical Information](#)

[Fusion Links](#)

Electromagnetic Analysis of ITER Diagnostic Equatorial Port Plugs during Plasma Disruptions

Y. Zhai^{1,a}, R. Feder¹, A. Brooks¹, M. Ulrickson², C. S. Pitcher³, G. D. Loesser¹

¹Princeton Plasma Physics Laboratory, Princeton, NJ, USA

²Sandia National Laboratory, Albuquerque, NM, USA

³ITER Organization, Route de Vinon sur Verdon, St Paul lez Durance, France

ITER diagnostic port plugs perform many functions including structural support of diagnostic systems under high electromagnetic loads while allowing for diagnostic access to the plasma. The design of diagnostic equatorial port plugs (EPP) are largely driven by electromagnetic loads and associate responses of EPP structure during plasma disruptions and VDEs. This paper summarizes results of transient electromagnetic analysis using Opera 3d in support of the design activities for ITER diagnostic EPP. A complete distribution of disruption loads on the Diagnostic First Walls (DFWs), Diagnostic Shield Modules (DSMs) and the EPP structure, as well as impact on the system design integration due to electrical contact among various EPP structural components are discussed.

I. INTRODUCTION

ITER diagnostic port plugs perform many functions including structural support of diagnostic systems under high electromagnetic loads while allowing for diagnostic access to the plasma [1]. Each water cooled generic port plug structure is filled with customized shielding and diagnostic equipment. The design of diagnostic equatorial port plugs (EPP) are largely driven by the electromagnetic loads and the associate responses of EPP structural components during fast plasma disruptions and VDEs [1-3]. To mitigate the large disruption loads, the design of diagnostic EPP has changed from the horizontal drawer configuration during conceptual design [4] to a vertical drawer configuration in the preliminary design [5-6] to effectively cut eddy current flowing paths on the EPP diagnostic drawers. As a result, a factor of 2-3 reduction of disruption loads brought down the maximum deflection of EPP structure during disruptions to <5 mm and the dynamic response of the EPP structure on the vacuum vessel becomes manageable. Although the upward major disruption with 36 ms linear current decay produces the largest radial moments and radial forces on the diagnostic first walls (DFWs), diagnostic shield modules (DSMs) and the EPP structure, other disruption cases or VDEs can produce larger minority disruption loads such as the poloidal moment and force. Electrical contact between DFWs and DSMs will also have a significant impact on the EM load distribution and thus affects the design of the DFW attachment scheme. Large current transfer (~160 kA) between DFWs and DSMs through the attachment keys and pads during disruption implies local heating and potential welding. A complete distribution of disruption

loads on the EPP structure and the associate responses, as well as impact on the system design integration due to electrical contact among various structural components will be discussed. A special technique for mapping the detailed disruption loads onto the EPP components from Opera EM analysis onto an ANSYS structural model is developed for an EM and structural mechanics integrated analysis [4-6].

Early conceptual design study indicates that electrical contact between the DSMs and the port plug structure may increase ~10-20% the net disruption loads on the full EPP structure [4]. The IO vertical drawer model includes a 5 mm gap between the front face of the EPP structure and the DSM. There will still be eddy current flowing between DSM and EPP structure through the rails and the DSM water pipes. To avoid potential arcing and welding, detailed analysis is performed to identify major eddy current loops and thus to quantify the current and voltages involved for potential arcing; also to extract disruption loads on the DFW and DSM cooling water pipes.

According to the Structural Design Criteria for ITER In-Vessel Components (SDC-IC), the major disruptions analyzed here are anticipated event and thus have a Level A load combination with a k factor of 1.

II. Model Description

A 20 degree sector of the ITER vacuum vessel (VV), the IO diagnostic vertical drawers with neighboring Blanket Shield Modules (BSMs), and the EPP structure is modeled in Opera 3d, a commercial electromagnetic analysis tool. The cyclic symmetric model uses the 3D Elecktra transient analysis capability of Opera 3d for the solution of eddy current problems on the EPP. Figure 1 presents the cutaway view of coils and plasma filaments modeled as secondary excitations. As shown in Figure 1, the central or vertical machine axis is aligned with the ITER global z axis. The machine mid-plane is on the X-Y plane with the X axis pointing to the radial direction. The 20-degree cut planes are symmetric around the vertical central X-Z plane. The EPP is 10 degrees off from the global X axis. A positive rotational symmetry around the global Z axis is applied to the Opera model with a total of 18 symmetry copies.

The 6 CS, 6 PF and 12 TF coil configuration is used to provide the static background field for force calculations during major disruptions. The ITER sign and direction convention is used so that plasma current and toroidal field are clockwise (-) but most CS and PF coils are counterclockwise (+). The plasma modeling based on the plasma simulation code DINA 2010 provides a transient history of plasma-induced flux change, a source excitation of eddy current in the model. The IO DINA 2010 data sets with 64 secondary excitations are used to model all plasma current drivers. The toroidal flux drivers are not included in the analysis as previous analysis indicated that it has a small impact on the EPP structure but will significantly increase the model run time [4-6]. The Halo current effect is also neglected since the present design of the EPP has 10 cm setback of the plasma-facing front face enforced to minimize this effect [1].

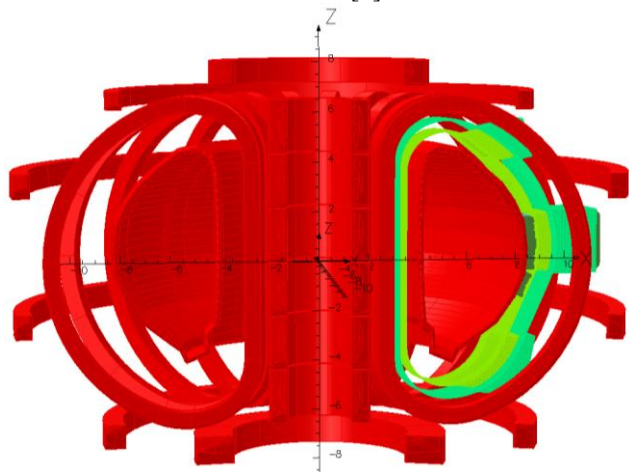


Figure 1 Cutaway view of the ITER coils and plasma filaments modeled as secondary excitations with a 20 degree model of VV and Diagnostic EPP (cyclic symmetry)

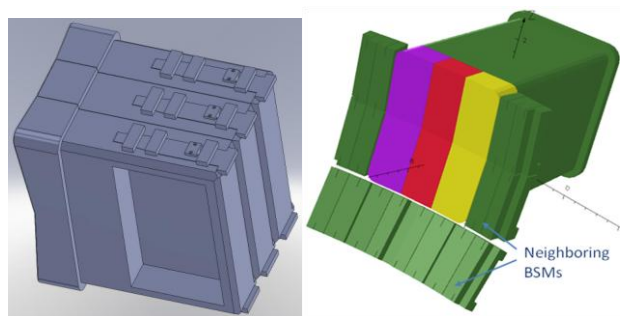


Figure 2 Vertical drawers and support rails (left) and Opera 3d model with the neighboring BSMs (right) of diagnostic equatorial port plug

The model background fields are benchmarked against results from ANSYS EMAG and Maxwell with generally

~3% difference. Figure 2 presents the IO vertical drawer model with support rails and Opera 3d model including neighboring BSMs. The upper neighboring BSM is not included here due to meshing difficulty. Table 1 presents the material conductivities used in the Opera 3d model.

Table 1 Electrical conductivity of the diagnostic EPP structural components

	Conductivity (S/m)
DFWs/DSMs	1.08×10^6 (80% SS)
Bolts and Pads	1.35×10^6 (SS)
Rails and EPP Structure	1.35×10^6 (SS)
Vacuum Vessel	1.35×10^6 (SS)

III. Disruption Scenarios

There are many ITER plasma disruption scenarios but the following cases listed in Table 2 are studied according to the IO requirements for CDR and PDR. As for potential category IV events, since we do not have detailed DINA simulation results, IO suggested two approaches 1) simply scale the EM loads for 26 ms disruption based on the loads from 36 ms disruption by a factor of $36/26=1.385$; 2) to run Opera model for 26 ms disruption case by accelerating the plasma current decay to 26 ms. This will be performed in future work and presented at the FDR.

Table 2 Selected Disruption Scenarios

VDE_UP_LIN36	VDE III (no VDE IV)	Level C
VDE_DW_LIN36	VDE III (no VDE IV)	Level C
MD_UP_LIN36	MD II (no MD III or MD IV)	Level A
MD_DW_LIN36	MD II (no MD III or MD IV)	Level A

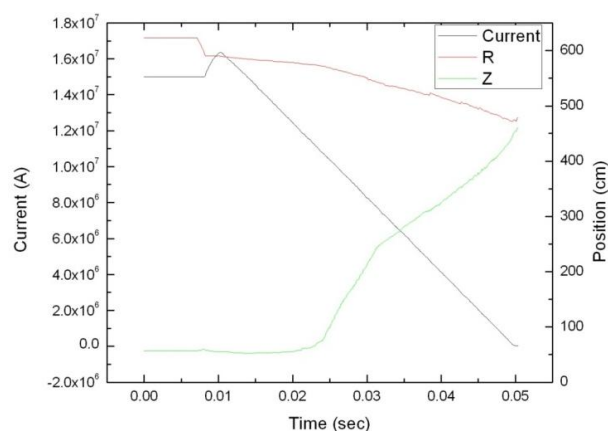


Figure 3 Plasma current and position during major upward disruption with 36 ms linear decay.

Figure 3 presents the total plasma current and its center position during major upward disruption with a 36 ms

linear current decay, which is the most important disruption case that gives the largest radial moment.

IV. Eddy Current Distribution

The eddy current distribution and resultant EM loads are summarized below for the four disruption cases listed in Table 2. Major disruption produces the largest radial force and radial moment on DFWs and the vertical drawers, but other disruptions may produce larger minority loads such as the vertical forces and vertical moments. Figure 4 presents the EPP eddy current distribution at the end of the major upward disruption with a 36 ms linear decay of plasma current.

The primary eddy current loops are 1) one big horizontal loop in the front part of each DFW/DSM, and front half of each vertical drawer 2) two big current loops on top and bottom of the EPP structure (not shown). The potential voltage of current loop on each drawer is estimated to be less than 25 V and the total current flowing in each eddy loop is over 100 kA.

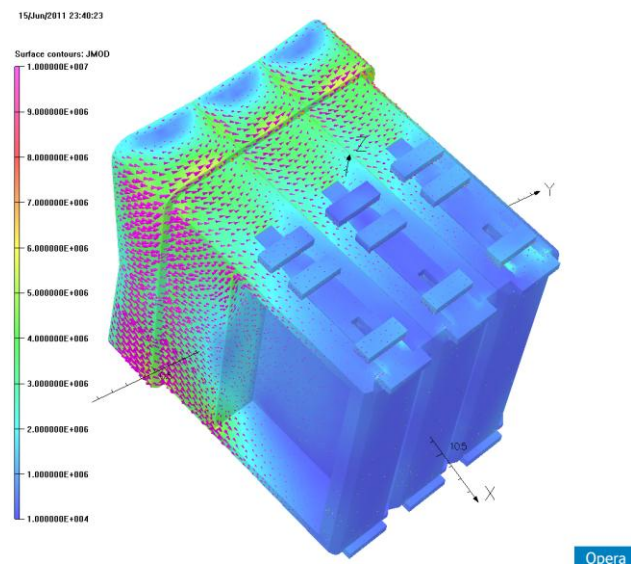


Figure 4 Eddy current distribution in DFWs and DSMs during MD_UP_LIN36.

To further validate the Opera model, Figure 5 presents the transient toroidal current flowing on the VV wall during disruptions. The net current is slightly less than the 15 MA plasma current mainly due to the conductive heat loss of the VV. The model global behavior indicates that the eddy current appears on the inner VV wall first before penetrating to the outer wall and the induced current is in the same direction as the plasma current flowing direction as we expected during plasma quench. Large amount of eddy current (~ 135 kA) will flow in the front top and

bottom of the EPP structure (~ 400 mm deep along the radial direction).

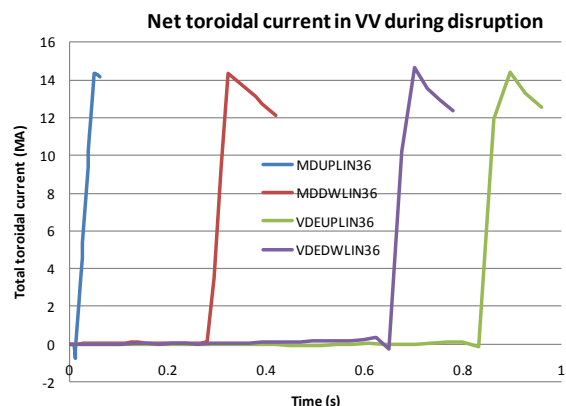


Figure 5 Net toroidal current induced in VV during disruptions.

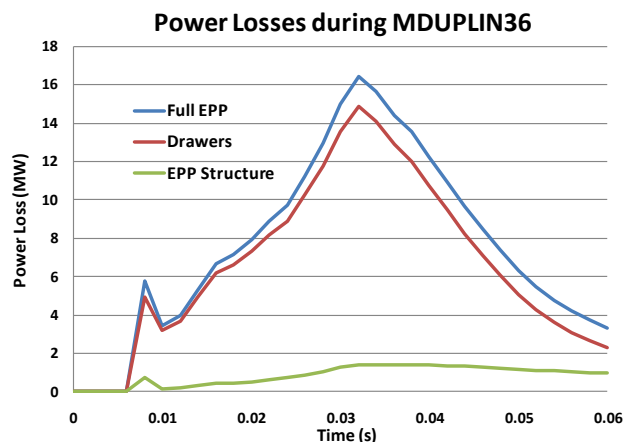


Figure 6 Total power losses in EPP structural components during MD_UP_LIN36.

The peak voltage of current loops on the EPP structure is ~ 25 V; the voltage difference between DSM and EPP structure is estimated to be less than 25 V. Figure 6 presents the total power losses during MDUPLIN36 for the model with no air gap between DFW and DSM. The net energy loss in the full EPP structure is ~ 500 kJ (90% on the drawer) and there is 60 kJ on the EPP structure and ~ 5 -6 kJ on top and bottom of the sliding rails.

VI. Disruption Loads

Eddy current induced forces are the volume integration of $J \times B$ force for each structural component. Since the full EPP structure is bolted at the end of the rear flange, the net disruption moment in the following results is given at the center of rear flange of the EPP structure with radial and poloidal coordinates $rc=11.5075$ m and $zc=0.62$ m respectively.

To minimize the electrical contact, a radial air gap between the DFWs and the EPP vertical drawers will reduce disruption loads on the DFWs and the full EPP structure. Radial force on the full EPP structure is reduced by 40% with an air gap and radial moment on the full EPP structure is reduced by 20%. Figure 7 presents a summary of peak EM loads on the full EPP structure during plasma disruptions and VDEs (four cases). The main observation is that unlike the radial moment all other load components change polarity during disruptions.

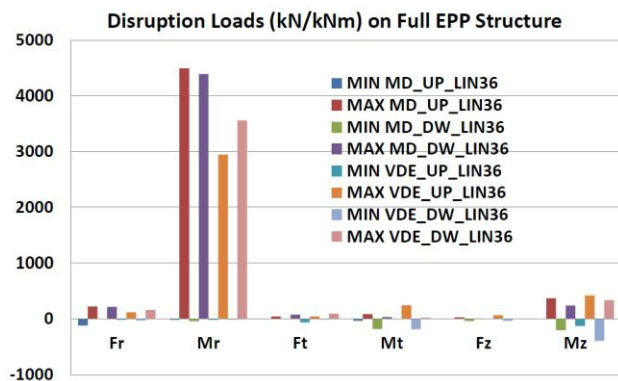


Figure 7 Disruption force and moment on the EPP for four disruption cases

Figure 8 presents a summary of peak EM loads on the vertical drawers during plasma disruptions and VDEs. MIN and MAX are the peak EM loads among all three vertical drawers during disruptions. The moment for each drawer is given at the mass center of the vertical drawer. The main observations are

1. The radial moment is still the dominant load, but the poloidal force is more significant than the radial force.
2. The toroidal and poloidal moments from VDE_DW_LIN36 are slightly larger than that from the MD_UP_LIN36 and MD_DW_LIN36.
3. The toroidal disruption loads are very small.
4. The radial moments do not change polarity during disruption while all the other loads do change polarity.

Positive radial forces on the drawers will push the drawer against the EPP structure and positive radial moments imply a torque of pointing away from the plasma twisting the drawers. The poloidal force on the two side vertical drawers (left and right looking from the plasma) tends to compensate each other.

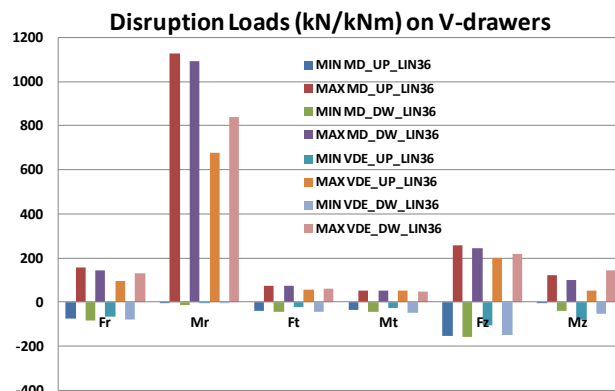


Figure 8 Disruption force and moment on EPP vertical drawers

An air gap between DFWs and DSMs has an important impact on the EM loads (both on the DFWs and on the full EPP structure). With a 2 mm air gap between DFWs and DSMs, the radial force on DFWs is reduced by a factor of 3; the radial moment is reduced by 18%, and the poloidal force is reduced by a factor of 2. Figure 9 listed the peak force and moment on DFWs during the major disruptions and VDEs.

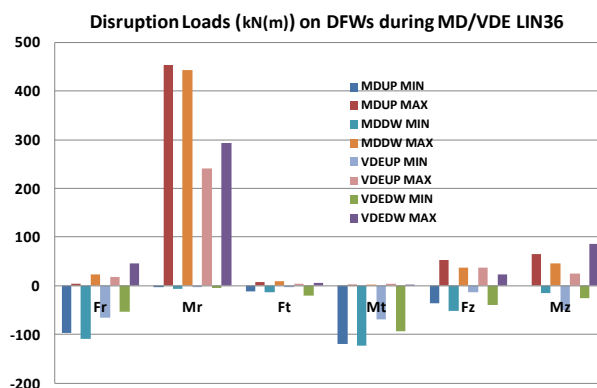


Figure 9 Disruption force and moment on the DFWs

VII. Response Implications

The design concept of DFW attachment scheme and mechanical integration of the DFWs with the drawers and EPP structure is validated by the static and dynamic response analysis. The DFWs are supported at interface with DSMs via keys and pads; the DSMs are supported on the EPP structure via the sliding rails, bolts and pins. The EPP structure is cantilevered at the port plug rear flange. A full dynamic analysis indicates a dynamic amplification factor of ~ 1.2 [1]. Figure 9 presents the total deflection of the full EPP structure under the Opera-ANSYS mapped static EM loading during MD_UP_LIN36. The EPP structure is simply twisted under the dominant radial

moment on the full EPP structure. The ~ 2 mm maximum deflection under the EM load only in the front face of DFWs is over a factor of 2 smaller than that from the horizontal drawer model due to the EM load reduction.

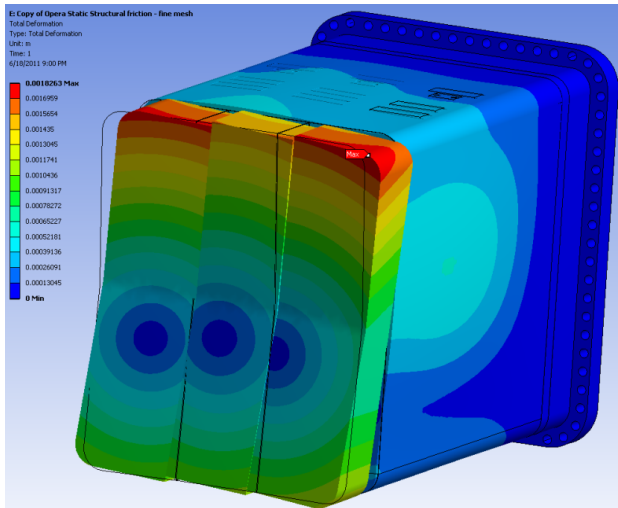


Figure 9 Total deflection of the full EPP structure.

VIII. Currents on Rails, Keys and Water Pipes

To qualify the current flowing between the DSMs and the EPP structure and the net current on other EPP structure components, we need to understand better the transient magnetic field. The eddy current at EPP is dominated by the transient poloidal field and the toroidal field (~ 4 T) is the dominant field at EPP for estimating the $J \times B$ forces. The transient B_z dot is ~ 15 T/s at the front face of EPP structure and it drops to 10 T/s at the mass center of the vertical drawer; it reduces further to less than 6 T/s at the back of the EPP structure.

To avoid local arcing and welding and to reduce EM force on water pipes, it is recommended to insulate the water pipes and diagnostic components. Due to the electrical contact with the EPP structure, eddy current flowing in the rails, pins/keys and DSM water pipes will not form a self-contained loop and this will potentially increase the net EM loads on these EPP components. Voltages on the rails and pins are estimated to be within a few volts.

A large amount of eddy current (10~30 kA) can flow in the bottom keys of the sliding rails during disruption, but only over a very short time frame. We need, however, to study potential welding at contact points between DSM and the rails in future work.

If no electrical contact with the EPP structure, there will be self-contained current loops on the vertical section of the water pipes and as a result, much smaller net EM

loads (the pipes are largely self-supported). With contact, however, large amount of eddy current (0.2-0.3 kA) on EPP back plate leaks into the pipes during disruptions and thus significantly increase the net $J \times B$ loads on the pipes (0.3-0.6 kN).

IX. CONCLUSIONS

Although major disruption produces the largest radial moments and radial forces on the vertical drawers and the full EPP structure, other disruption cases or VDEs can produce a larger minority load such as the poloidal moment and force.

The radial moment on the drawers is dominant but poloidal force is as significant as the radial force on the drawer. Toroidal and poloidal moments from VDE_DW_LIN36 are slightly larger than that from the major disruptions. The dominant radial moments do not tend to change polarity during disruption and VDE but all other load components do.

ACKNOWLEDGMENTS

This work is supported by DOE contract numbers DE-AC02-09CH11466 (PPPL) and DE-AC05-00or22725 (UC-Battelle, LLC). The views and opinions expressed herein do not necessarily reflect those of the ITER Organization.

REFERENCES

1. C. S. Pitcher et al, "Port-Based plasma diagnostic infrastructure on ITER", TOFE-2012, to be published in Fusion Science and Technology, 2012.
2. L. Doceul et al, "CEA engineering studies and integration of the ITER diagnostic port plugs", Fusion Engineering and Design, **82** 1216-1223, 2007.
3. L. Meunier et al, "Engineering activities on the ITER representative diagnostic equatorial port plug", Fusion Engineering and Design, **84** 1294-1299, 2009.
4. Y. Zhai and R. Feder, "Equatorial port plug transient electromagnetic and structural analysis during major disruption with 36 ms linear decay", ITER Report, December, 2010.
5. Y. Zhai et al, "Diagnostic equatorial port plug transient electromagnetic analysis during plasma disruptions and VDEs", ITER Report 4KXA57 v1.1, July, 2011.
6. Y. Zhai et al, "ITER Diagnostic First Wall CDR – Transient electromagnetic, static structural and thermal fatigue analysis", ITER Report, June, 2011.
7. A. Brooks, "EM analysis of the generic upper port plug diagnostic", ITER Report 348DL, May, 2010.

The Princeton Plasma Physics Laboratory is operated
by Princeton University under contract
with the U.S. Department of Energy.

Information Services
Princeton Plasma Physics Laboratory
P.O. Box 451
Princeton, NJ 08543

Phone: 609-243-2245
Fax: 609-243-2751
e-mail: pppl_info@pppl.gov
Internet Address: <http://www.pppl.gov>